Available online at www.sciencedirect.com
SCIENCE DIRECT®
Physica E 18 (2003) 523–529
PHYSICA E
www.elsevier.com/locate/physe

Single-electron charging spectra: from natural to artificial atoms

B. Szafran*, P. Sęp, J. Adamowski, S. Bednarek

Faculty of Physics and Nuclear Techniques, AGH – University of Science and Technology, al. Mickiewicza 30, Kraków 30-059, Poland

Received 6 March 2003; accepted 4 April 2003

Abstract

We present a theoretical study of the charging spectra in natural and artificial atoms. We apply a model electrostatic potential created by a homogenously charged sphere. This model potential allows for a continuous passage from the Coulomb potential of the nucleus to parabolic confinement potential of quantum dots. We consider electron systems with $N = 1, \ldots, 10$ electrons with the use of the Hartree–Fock method. We discuss the qualitative similarities and differences between the chemical potential spectrum of electron systems bound to nucleus and confined in quantum dots.

PACS: 73.21.−b. 13.10.+z

Keywords: Quantum dots; Artificial atoms; Hartree–Fock method

1. Introduction

The three-dimensional confinement of electrons in semiconductor quantum dots [1] results in a discrete atomic-like quantization of energy levels. For this reason the electron systems in quantum dots are called artificial atoms [2].

Besides the discrete energy spectrum the artificial and natural atoms exhibit similar capability of binding the many-electron systems. The existence of a stable N-electron atom (or ion) is possible if the chemical potential of N-electron system, defined as $\mu_N = E_N - E_{N-1}$, where E_N is the N-electron ground state energy, does not exceed the continuum threshold energy. Absolute value of μ_N is equal to the energy released when an additional electron is bound to the atom (or ion). For natural atoms the continuum threshold is determined by the minimal energy of an unbound electron state, while for artificial atoms it can be identified with the Fermi energy of the electron reservoir (electrode) which is the source of electrons. Basic experiments testing the properties of natural and artificial atoms consist in measurement of single-electron charging, i.e. in a direct or indirect determination of the chemical potentials. The absolute values of chemical potential of natural atoms (and ions) define the ionization energy, which is measured in photoionization processes. The single-electron charging of quantum dots is observed in transport [3] or capacitance [4] spectroscopy. The ionization energies of natural atoms exhibit a distinct shell structure. In quantum dots the shell filling can be observed [5,6] if the energy spacings between the single-electron energy levels are at least of the order of electron–electron interaction energy, i.e. if the size of the dot is small enough.

The binding of electrons in natural atoms is due to the Coulomb attraction by the nucleus. The potential that binds the excess charge carriers in quantum

* Corresponding author. Tel.: +4812-6172974; fax: +4812-6340010.
E-mail address: bszafran@agh.edu.pl (B. Szafran).

1386-9477/03/$ - see front matter
doi:10.1016/S1386-9477(03)00268-6

dots is called a confinement potential. The confinement potential in quantum dots may result from various physical effects and posses different symmetry and profile in different nanostructures [1,3,7]. However, in most of calculations the parabolic potential [8–16] is used. The aim of the present study is to investigate the charging spectra determined by chemical potentials, for natural atoms (and ions) as well as for artificial atoms with parabolic confinement potential. This investigation provides a comparative study of the fundamental property of natural and artificial atoms, namely their capability of binding the charge carriers. For this purpose, we use a spherically symmetric model of the confinement potential which allows for a smooth passage from the Coulomb to parabolic potential [17]. Most of the quantum dots are flat [1,3,7], so the spherical symmetry of these nanostructures is rather a rare feature. Nevertheless, quantum dots with nearly spherical shape are produced [7] as nanocrystals in an organic or insulating matrix.

The study of the charging spectra requires the few-electron Schrödinger equation to be solved. The problem of few-electron system confined in quantum dots can be treated by the Hartree–Fock method [8–11,18–20], exact diagonalization schemes [12,21,13–15] or density functional approach [16,22–24]. In this paper, we use the Hartree–Fock method, which allows for the description of the charging spectra and shell filling effects in quantum dots [19,20]. These effects appear for quantum dots with intermediate and small sizes. In the case of these dots the Hartree–Fock method works with a reliable precision, although for larger structures it can predict erroneous ground-state symmetry [15]. The HF is also known [25] to reproduce with a high precision the ionization energies of natural atoms and ions.

This paper is organized as follows: in Section 2 we present the model confinement potential, the solutions of one-electron and describe the method of solution of the few-electron problem, the results and discussion are given in the Section 3, Section 4 provides conclusion and summary.

2. Theory

The study which is the aim of the present paper requires a model confinement potential flexible enough to reproduce the Coulomb potential of the nucleus as well as the parabolic confinement potential of quantum dots. Moreover, this model should allow for a continuous transition between the two ideal limit cases. The potential which fulfills these requirements is the spherically symmetric electrostatic potential created by a charge spread homogenously over the volume of a sphere

$$V(r) = \begin{cases} \frac{1}{2}\frac{Zr^2}{R^3} - \frac{3}{2}\frac{Z}{R} & \text{for } r < R, \\ -\frac{Z}{r} & \text{for } r > R, \end{cases} \tag{1}$$

where R is the radius of the sphere and Z is its charge. In formula (1) and in the rest of the paper we use the atomic units, i.e. we use the Bohr radius as the distance unit and the Hartree unit for the energy. Potential (1) is the electrostatic potential of positive background charge. For semiconductor quantum dots this interpretation should be taken with caution, since there is no positive background in these structures. The quantum dots confine the conduction band excess electrons. Therefore, they are not neutral, but negatively charged. Two-dimensional version of potential (1) has been used [26] as a model confinement potential of disk-like quantum dots. Bielińska-Wąż et al. [27] have studied the two-electron system in a spherically-symmetric superposition of Coulomb and parabolic potentials.

Let us look at the shape of potential (1). The thick solid lines in Fig. 1 show the confinement potential (1) for $R = 0.5$ and $R = 1$. Here, and in the rest of the paper we take $Z = 10$, which corresponds to the atom of neon and its ions. The dotted line presents the Coulomb potential $V_c = -10/r$. The thin vertical lines show the surface of the charged sphere for $R = 0.5$ and 1. For finite values of R potential (1) does not possess a singularity at the origin, it is parabolic inside the sphere ($r < R$) and reduces to Coulomb potential in the outside ($r > R$). The broken lines show the one-electron ground-state radial probability densities ($r^2|\psi(r)|^2$) for $R = 0.5$ and $R = 1$. The probability densities were obtained by solving the one-electron Schrödinger equation with a finite-difference method. The broken curves were shifted by an arbitrary constant for aesthetic reasons. When the radius of the sphere increases, the probability of finding the particle outside the sphere decreases (it is 28% for $R = 0.5$ and 12% for $R = 1$, respectively). This means that for

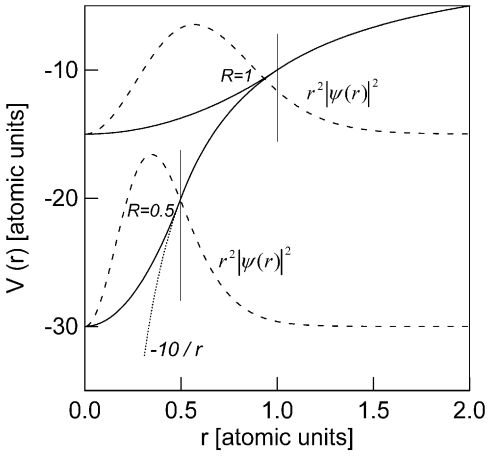

Fig. 1. Confinement potential [Eq. (1)] for $Z = 10$, $R = 0.5$ and $R = 1$ (solid lines) and the Coulomb potential $(-10/r)$ (dotted line). The single electron-ground state radial probability density $(r^2|\psi(r)|^2)$ for $R = 0.5$ and $R = 1$, shifted by an arbitrary constant (broken lines). The vertical lines mark the surface radii of the two spheres. The quantities of r and $V(r)$ are expressed in atomic units.

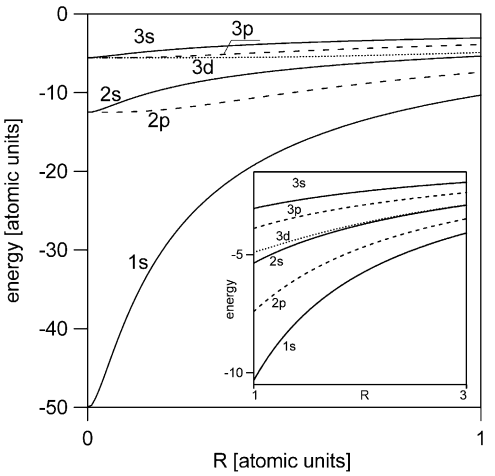

Fig. 2. One-electron energy spectrum for potential (1) as function of the radius of the charged sphere (R). The solid lines show the s energy levels, broken lines show the p levels and dotted line show the 3d level. The inset displays the spectrum for larger values of R. The atomic units are used.

sufficiently large radius of the sphere the electron feels only the parabolic part of the confinement potential. This effect occurs also for excited-state wave functions and makes the model potential (1) a suitable one for the purpose of the present study. The transition from the Coulomb potential to the harmonic confinement can be performed by tuning the value of the radius of the charged sphere R.

The evolution of the one-electron energy spectrum with R is displayed in Fig. 2. We use the standard atomic notation and display 1s,2s,3s,2p,3p, and 3d energy levels. For $R = 0$ the energy spectrum is the hydrogen-like spectrum of Ne^{9+} ion. When R increases from zero, all the energy levels increase. This increase is the strongest for the states of s symmetry, whose wave functions do not vanish at the origin. The wave functions corresponding to states with non-zero angular momentum react with a certain delay at the change of the potential near the origin. This results in lifting the degeneracy of 2s,2p as well as 3s,3p,3d levels of hydrogen-like ion. The inset of Fig. 2 shows the same energy levels for larger values of R. We see that in the large R limit the spacings between the energy levels become constant. Moreover, the first excited state is of p symmetry, the second excited state is composed of degenerate 2s and 3d states. In this way, the hydrogen energy spectrum evolves into the harmonic oscillator spectrum when R is increased.

In order to determine the charging spectrum of natural and artificial atoms we have to solve the N-electron Schrödinger equation for the ground state. The Hamiltonian of the system reads

$$H = \sum_{i=1}^{N} \left(-\frac{\nabla_i^2}{2} + V(r_i) + \sum_{j>i}^{N} \frac{1}{r_{ij}} \right). \quad (2)$$

The N-electron ground state is determined with the spin-unrestricted Hartree–Fock method. The one-electron trial wave functions are developed in the Gaussian basis

$$\psi_{k,s}(r) = \sum_{j=1}^{J} \sum_{i_1,i_2,i_3=0}^{i_1+i_2+i_3 \leqslant 1} c_{i_1,i_2,i_3,j}^{k,s} x^{i_1} y^{i_2} z^{i_3} \exp(-\alpha_j r^2), \quad (3)$$

where s stands for the value of the z-component of the electron spin, k numbers the orbital for a given s, $c_{i_1,i_2,i_3,j}^{k,s}$ are linear variational parameters, α_j are the nonlinear variational parameters, and J is the number of nonlinear parameters used. Basis (3) allows for construction of s and p symmetry one-electron wave functions, which is sufficient for the description of the ground states with N up to 10.

In the present calculations we apply $J = 12$ nonlinear variational parameters. Gaussian basis (3) cannot reproduce exactly the hydrogen-atom wave functions, but it reproduces exactly the lowest harmonic oscillator eigenfunctions. Therefore, the convergence of the total energy estimates with respect to the size of the basis is faster for non-zero R values. For $J = 12$ basis (3) contains 48 elements and yields -128.518 for the total ground-state energy of neutral Ne atom, while the exact HF result is -128.547 [25]. We have estimated that the ground state energy of the artificial Ne with $R = 2$ is determined with a precision of 10^{-3} atomic units.

3. Results and discussion

Fig. 3 shows the calculated chemical potentials for the systems with $N = 1, \ldots, 10$ electrons as functions of the radius of the charge sphere R. The values for $R = 0$ correspond to the ionization energies of Ne ions. These ionization energies form two groups

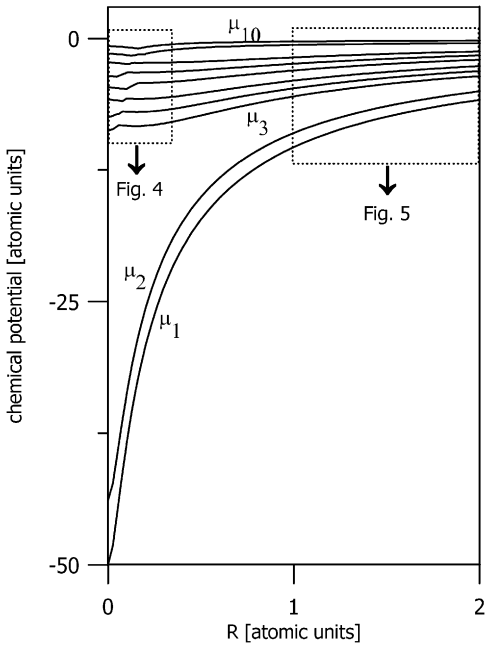

Fig. 3. Evolution of the charging spectrum when passing from natural to artificial atoms. Chemical potentials μ_N for $N = 1, \ldots, 10$. The atomic units are used.

with distinctly different values. The energy needed to remove 1s electron from Ne^{8+} ($\Delta E = -\mu_2$) and Ne^{9+} ($\Delta E = -\mu_1$) ions is much larger than the ionization energies for 2s and 2p valence electrons of less charged ions. This results from the fact that in the natural ions the binding energies of electrons from different shells are of different orders of magnitude. The chemical potentials grow when R increases, which is related to analogous dependence of the single-electron energy levels presented in Fig. 2. The first and second electrons occupy 1s level, which reacts more rapidly on the change of the potential near the origin than 2s and 2p energy levels. In consequence, the chemical potentials of one and two-electron systems increase much faster with R than the chemical potentials of systems containing three to ten electrons. For large values of R the difference between the ionization energies diminishes. We note, that in particular the difference between μ_2 and μ_1 is decreased. This difference can be interpreted as the electron–electron interaction energy in the two electron system. The decrease of the electron–electron interaction energy results from increase of the system size when R is increased. The spin-orbital configurations given at the right-hand side of Fig. 4 are the final ones, i.e. they do not change any more as R increases further.

A closer inspection of the chemical potentials of electron-systems with three to ten electrons exhibits characteristic deviations from monotonous dependence for values of R from 0 to about 0.3. Fig. 4 shows this interesting aspect of our results. We remind, that for $R = 0$ the results correspond to the ionization energies of natural Ne ions. The open circles mark the experimental data for these quantities. A look at the differences between the adjacent chemical potentials defined as addition energy $\Delta_N = \mu_{N+1} - \mu_N$ reveals the shell-filling mechanism in natural ions. This quantity is particularly large for N which fills a shell or a subshell. For zero radius of the charge sphere Δ_4 and Δ_7 are larger than the other addition energies. This is because the fourth electron fills the 2s shell and because the seven-electron system corresponds to a half-filled 2p shell, in which all the three electrons posses parallel spins. The relatively large value of Δ_7 is results from the exchange interaction, and is a signature of the Hund rule.

In Fig. 4 the orbital configurations of N-electron system are given below the line corresponding to

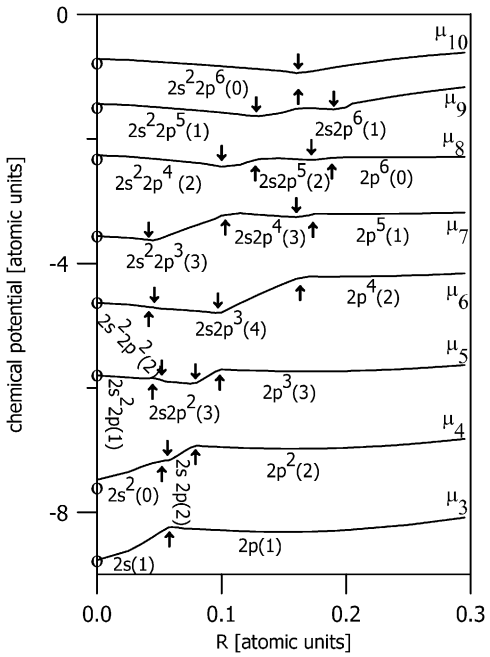

Fig. 4. Zoom of the upper left fragment of Fig. 3. The ground state transformations in $N=3,\ldots,10$ electron systems. The orbital configuration of valence electrons in the N-electron ground state is given under the line corresponding to μ_N (in all the systems the 1s level is doubly occupied). The value of the total spin z-component in $\hbar/2$ units is given in parentheses next to the orbital configuration. The up (down) arrows show the cusps of μ_N line corresponding to the ground-state transformation of N $(N-1)$ electron system. The open circles for $R=0$ mark the experimental values of the ionization energies of Ne ions.

μ_N. For each orbital configuration the ground state corresponds to the maximal allowed value of the total spin. The values of the total spin z-component are given (in $\hbar/2$ units) in parentheses after the specification of the orbital configuration. In all the systems presented in Fig. 4, the 1s energy level is doubly occupied, and this information is omitted in the figure. When R increases from zero, the 2s energy level grows faster than the 2p level (c.f. Fig. 2). In consequence for certain radii of the sphere the ground-state is degenerate, i.e., there are two different spin-orbital configurations corresponding to the same ground-state energy. A change of R from the values corresponding to this degeneracy results in the changes of the electronic spin-orbital configurations of the ground state. The transformations of the ground state symmetry of N-electron system are accompanied by cusps of chemical potentials μ_N and μ_{N+1} as functions of R. The cusps on μ_N lines are marked by arrows pointed up and the cusps on μ_{N+1} lines are marked by arrows pointing down. In consequence of these transformations the 2s shell is left empty in electron systems containing up to 8 electrons. In three- and nine-electron systems there appears a single ground-state transformation when one of the electrons from the 2s shell passes to 2p shell. In the systems with four to eight electrons the 2s electrons pass to 2p shell one by one. Therefore, for these systems there appear two transformations of the ground state. The ones which appear for smaller values of R will be referred to as 'first' and the ones appearing for larger values of R will be referred to as 'second'. The ground state configuration of ten electron system remains unchanged when R is increased.

The exchange interaction has a visible influence on the values of the critical radii which induce the ground-state transformations. The first transformations for $N=4,5$ and 6 increase the spin state of the system and the values of R corresponding to these transformations are the smallest, because these transformations are favored by the exchange interaction. The second transformations for $N=6,7$ and 8 reduce the value of the spin, and the corresponding R values are relatively large, since the exchange interaction inhibits these transformations. The other transformations leave the spin-state unchanged.

Fig. 5 shows the chemical potential spectrum for values of R between 1 and 2. This spectrum is qualitatively similar to that of harmonic oscillator confinement potential. The electrons fill the subsequent shells 1s, 2p and 2s. Certain addition energies are larger than the others in a characteristic manner. Namely, the large values of Δ_2 and Δ_8 are related to the filling of 1s and 2p shell, respectively. Large value of Δ_5 is a signature of the Hund rule, i.e. half-filling of the 2p shell.

In the harmonic-oscillator limit the shell-filling mechanism is similar to that in the natural atom: the electrons occupy subsequent shells, in each case the ground state corresponds to maximum value of the total spin. However, the order of occupied shells is different in natural and artificial atoms, which for values of $N \leqslant 10$ studied in the present paper can be explained by the order of single-electron energy levels. The single-electron spectrum for $R=0$ exhibits the degeneracy of 2s and 2p energy levels.

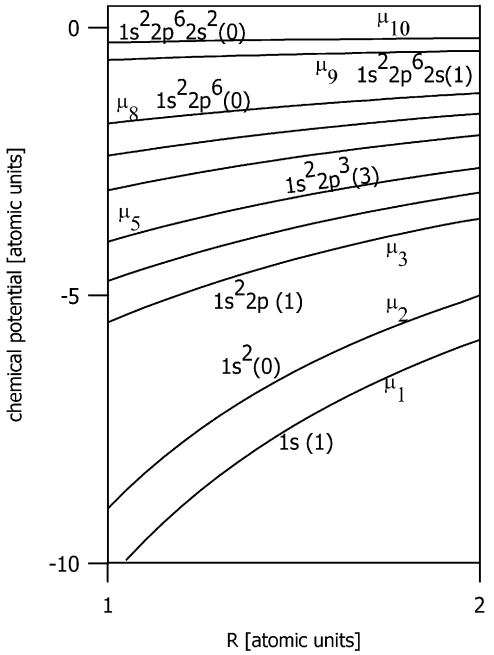

Fig. 5. Zoom of the upper right fragment of Fig. 3. The orbital configurations and the values of z-component of the total spin are given in $\hbar/2$ units.

This degeneracy is lifted in few-electron systems, and the electrons first occupy 2s shell and next the 2p energy level. In the limit of large values of R the 2s energy level is degenerate with the 3d energy level. We have performed additional calculations with basis extended to cover the d symmetry. We have verified in this way that the 9th and 10th electrons occupy the 2s shell, and 3d shell is left empty in the ground state of nine- and ten-electron systems. In the case of both natural and artificial atoms the electrons occupy this of degenerate energy levels which corresponds to lower angular momentum.

In the evolution of the charging spectrum from natural to artificial atoms we have found a region when the regular shell-filling mechanism is broken, i.e. the range of R in which the electrons occupy both 2s and 2p energy level while none of these shells is completely filled (c.f. Fig. 4). These states which violate the Hund rule, appear in 4–8 electron systems in the range of R between the two ground-state transformations.

4. Conclusion and Summary

We have performed a theoretical study of the evolution of the charging spectra when passing from natural to artificial atoms. We have used a model confinement potential of a positively charged sphere which allows for a smooth transition from the Coulomb to parabolic potential. We have shown that the ground-state of few-electron systems undergoes several ground-state transformations associated with a change of the symmetry when the potential is changed from Coulomb to parabolic. The order of these transformations is in a visible way affected by the spin effects. We have also shown that—although the natural and artificial atoms exhibit a similar shell filling mechanism—the charging spectrum of the artificial atoms is affected by the shell structure in a much smaller extent than that of natural atoms. We have found that the simple shell filling mechanism of natural and artificial atoms is violated in the size-regime in which the ground-state transformations appear.

Acknowledgements

This paper is supported in part by the Polish Government Scientific Research Committee (KBN).

References

[1] L. Jacak, P. Hawrylak, A. Wójs, Quantum Dots, Springer, Berlin, 1998.
[2] P.A. Maksym, T. Chakraborty, Phys. Rev. Lett. 65 (1990) 108.
[3] L.P. Kouwenhoven, D.G. Austing, S. Tarucha, Rep. Prog. Phys. 64 (2001) 701.
[4] R.C. Ashoori, N.B. Zhitenev, L.N. Pfeiffer, K.W. West, Physica E 3 (1998) 15.
[5] S.Tarucha, D.G. Austing, T. Honda, R.J. van der Hage, L.P. Kouwenhoven, Phys. Rev. Lett. 77 (1996) 3613.
[6] B.T. Miller, W. Hansen, S. Manus, R.J. Luyken, J.P. Kotthaus, S. Huant, G. Medeiros-Ribeiro, P.M. Petroff, Phys. Rev. B 56 (1997) 6764.
[7] A.D. Yoffe, Adv. Phys. 50 (2001) 1.
[8] H.M. Müller, S.E. Koonin, Phys. Rev. B 54 (1996) 14532.
[9] C. Yannoulenas, U. Landman, Phys. Rev. Lett. 82 (1999) 5325.
[10] B. Reusch, W. Häusler, H. Grabert, Phys. Rev. B 63 (2001) 113,313.
[11] M. Fujito, A. Natori, H. Yasunaga, Phys. Rev. B 53 (1996) 9952.

[12] M. Eto, Jpn. J. Appl. Phys. 36 (1997) 3924.
[13] S.R.E. Yang, A.H. MacDonald, Phys. Rev. B 66 (2002) 041304.
[14] M. Manninen, S. Viefers, M. Koskinen, S.M. Reimann, Phys. Rev. B 64 (2001) 245322.
[15] B. Szafran, J.Adamowski, S. Bednarek, Physica E 5 (2000) 185.
[16] S.M. Reimann, M. Koskinen, M. Manninen, B.R. Mottelson, Phys. Rev. Lett. 83 (1999) 3270.
[17] S.N. Klimin, V.M. Fomin, F. Brosens, J. Devreese, unpublished.
[18] S. Bednarek, B. Szafran, J. Adamowski, Phys. Rev. B 59 (1999) 13036.
[19] B. Szafran, J. Adamowski, S. Bednarek, Phys. Rev. B 61 (2000) 1971.
[20] S. Bednarek, B. Szafran, J. Adamowski, Phys. Rev. B 64 (2001) 195303.
[21] D. Pfannkuche, V. Gudmundsson, P.A. Maksym, Phys. Rev. B 47 (1993) 2244.
[22] O. Steffens, M. Suhrke, U. Rőssler, Physica B 256–258 (1998) 147.
[23] P. Matagne, J.P. Leburton, Phys. Rev. B 65 (2002) 235323.
[24] M. Pi, A. Emperador, M. Barranco, F. Garcias, K. Muraki, S. Tarucha, D.G. Austing, Phys. Rev. Lett. 87 (2001) 066801.
[25] B.Y. Tong, L.J. Sham, Phys. Rev. 144 (1966) 1.
[26] A.S. Mikhailov, Physica E 12 (2002) 884.
[27] D. Bielińska-Wąż, J. Karwowski, G.H.F. Diercksen F, J. Phys. B. At. Mol. Opt. 34 (2001) 1987.